# Disorder Influence on Linear Dichroism Analyses of Smectic Phases

Joshua Manor,* Ziad Khattari,† Tim Salditt,† and Isaiah T. Arkin*
*Department of Biological Chemistry, The Alexander Silberman Institute of Life Sciences, The Hebrew University of Jerusalem, Jerusalem, Israel; and †Institut für Röntgenphysik, Georg-August-Universität Göttingen, Göttingen, Germany

ABSTRACT Linear dichroism, the unequal absorption of parallel and perpendicular linear polarized light, is often used to determine the anisotropic ordering of rodlike polymers in a smectic phase, such as helices in a lipid bilayer. It is a measure of two properties of the sample: 1), orientation of the chromophore transition dipole moment (TDM) and 2), disorder. Since it is the orientation of the chromophore TDM that is needed for high resolution structural studies, it is imperative to either deconvolve sample disorder, or at a minimum, estimate its effect upon the calculated TDM orientation. Herein, a rigorous analysis of the effects of disorder is undertaken based on the recently developed Gaussian disorder model implemented in linear dichroism data. The calculation of both the rod tilt and rotational pitch angles as a function of the disorder and dichroism, yield the following conclusions: Disorders smaller than 5° have a vanishingly small effect on the calculated polymer orientation, whereas values smaller than 10° have a negligible effect on the calculated parameters. Disorders larger than 10° have an appreciable effect on the calculated orientational parameters and as such must be estimated before any structural characterization. Finally the theory is tested on the HIV vpu transmembrane domain, employing experimental mosaicity measurements from x-ray reflectivity rocking scans and linear dichroism.

## INTRODUCTION

The level of anisotropic ordering of rodlike polymers in a smectic phase is of significant importance in many systems, including biological environments. For example, knowledge of the tilt of a transmembrane helix relative to the lipid bilayer normal often represents a first stage toward characterizing the structure of a protein.

One of the more powerful tools to analyze the level of anisotropic ordering is linear dichroism spectroscopy. The angle between the polymer director and the smectic phase principle axis is then readily derived, based on the knowledge of the geometry relating the transition dipole moment (TDM) of the absorbing chromophore, to the polymer axis. The reader is referred to a comprehensive review by Axelsen and Citra (1). For example, in $\alpha$-helices the angle between the director and the TDM of the amide I vibrational mode (mostly the C=O stretch) is 39° (2,3). Note that according to Fig. 1, $\alpha$ of the amide I vibrational mode is in fact 180°–39° = 141°.

The above, however, is only true in homogeneous systems in which all polymers are tilted from the smectic phase principle axis by the same amount. Any deviation from homogeneity will immediately influence the measured dichroism, thereby diminishing its information content and respective analytical utility. It is for this reason that dichroism measurements routinely yield an order parameter, $\mathcal{S}$, which reflects the nonlinear, average distribution of the polymer tilt angle, $\theta$, rather than a direct angle:

$$\mathcal{S} = \frac{3\langle\cos(\theta)^2\rangle - 1}{2}. \quad (1)$$

The expression is the second-order Legendre polynomial as discussed in Axelsen and Citra (1). In many instances, such as structural analyses of membrane proteins, an order parameter is of little use, since what is needed is an explicit angle between the helix director and the membrane normal.

To overcome the above problem it is necessary to deconvolve the sample disorder, and its influence upon the measured dichroism, or at a minimum estimate its effect. For this reason we have undertaken a computational approach aimed at estimating the effect of sample inhomogeneity on the measured dichroism and its effect upon the calculated orientation of transmembrane helices. Three vibrational modes (Protein Amide I and Amide A and Lipid $CH_2$ stretching modes) were tested for the effect of disorder on the helix tilt orientation. In addition, four different helix tilt orientations were used to estimate the effect of the disorder on the orientation pitch angle of a specific site on the helix.

## THEORY

### Geometric definitions

The spatial orientation of a chromophore TDM located in a rodlike polymer, with respect to a smectic phase principal axis, can be described using a set of four angles following Fraser (4,5), as shown in Fig. 1:

1. $\beta$ – The tilt angle of the rod with respect to the smectic phase principal axis. In this instance it is the $z$ axis. Thus the sample is uniaxially symmetrical in the $x$,$y$ plane (due to the peptide solubility in the bilayer). When the polymer is a rigid rod, $\beta$ assumed to be constant for all amino acids along the rod (or polymer).

*Submitted December 30, 2004, and accepted for publication April 6, 2005.*

Address reprint requests to Isaiah T. Arkin, Tel./Fax: 972-2-658-4329; E-mail: arkin@cc.huji.ac.il.



0006-3495/05/07/563/09 $2.00

doi: 10.1529/biophysj.104.058842

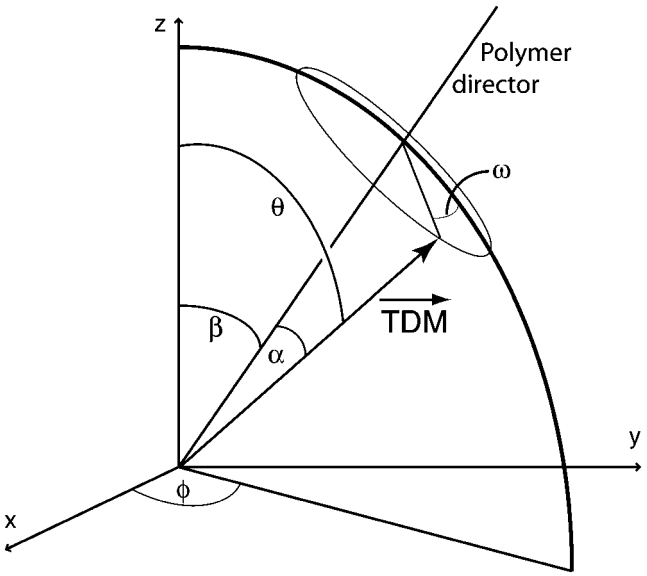


FIGURE 1 Schematic diagram of a chromophore transition dipole moment (*TDM*) located on a rodlike polymer that rotates in uniaxial symmetry about the $z$ axis.

2. $\phi$ – The rotation of the rod about the smectic phase principal axis.
3. $\alpha$ – The angle between the chromophore TDM and the rod director.
4. $\omega$ – The rotational pitch angle of the chromophore TDM about its director. It is defined as 0° when the helix's director, the membrane normal, and the transition dipole moment all reside in the same plane.

When dealing with a uniaxially symmetric smectic phase, as is the case in transmembrane $\alpha$-helices, the rotational angle of the protein of interest, $\phi$, is considered to be random for each protein due to uniaxial symmetry.

## Dichroic ratio

The dichroic ratio, denoted by $\mathcal{R}$, is the quotient of the parallel-polarized light absorption, $A_{\parallel}$, and the perpendicular-polarized light absorption, $A_{\perp}$:

$$\mathcal{R} \equiv \frac{A_{\parallel}}{A_{\perp}}. \tag{2}$$

The absorption of light is equal to the squared scalar product of the axial electric field components: $\mathcal{E}_x$, $\mathcal{E}_y$, and $\mathcal{E}_z$ (see Appendix), and the corresponding integrated, dimensionless absorption coefficients: $\mathcal{K}_x$, $\mathcal{K}_y$, and $\mathcal{K}_z$. Considering this notation, in the geometrical configuration of attenuated-total reflection Fourier transform infrared (ATR-FTIR), as shown in Fig. 2, the dichroism is equal to (6)

$$\mathcal{R}^{\mathrm{ATR}} = \frac{\mathcal{E}_z^2 \mathcal{K}z + \mathcal{E}_x^2 \mathcal{K}z}{\mathcal{E}_y^2 \mathcal{K}y}. \tag{3}$$

There are two types of dichroic ratios measured in ATR-FTIR – the polymer dichroic ratio, $\mathcal{R}_{\mathrm{polymer}}$, and the site dichroic ratio, $\mathcal{R}_{\mathrm{site}}$:

1. $\mathcal{R}_{\mathrm{polymer}}$ refers to the dichroism of the unlabeled vibrational modes that are distributed randomly about the polymer director. It is normally used to extract the tilt angle of the polymer backbone.
2. $\mathcal{R}_{\mathrm{site}}$ refers to the dichroism at a certain isotope-edited site. It is used to extract the rotational pitch angle of the labeled site. Taken together, $\mathcal{R}_{\mathrm{polymer}}$ and $\mathcal{R}_{\mathrm{site}}$ can be used to determine all geometrical parameters of a rigid polymer, if the sample disorder is known.

## Sample disorder

In any system, and in certain biological samples, a variation in the tilt angle of the polymer is to be expected. Fraser (4) proposed a simple model for the influence of the disorder, in which the desired function describing the dichroic ratio is

$$\mathcal{R} = \frac{\mathcal{E}_z^2\left(f\mathcal{K}_z + \frac{1-f}{3}\right) + \mathcal{E}_x^2\left(f\mathcal{K}_x + \frac{1-f}{3}\right)}{\mathcal{E}_y^2\left(f\mathcal{K}_y + \frac{1-f}{3}\right)}, \tag{4}$$

where $f$ denotes the perfectly ordered fraction of material and $1 - f$ denotes the random fraction. However, as proposed later by Fraser (5), a better disorientation model might utilize a distribution function. Kass et al. (7) proposed a Gaussian distribution for the approximation of the helices tilt from the lipid bilayer. According to this, the expression of the dichroism must therefore be changed to

$$\mathcal{R} = \frac{\mathcal{E}_z^2 \int_{-\infty}^{\infty} F\{\beta\}\,\mathcal{K}z\,d\beta + \mathcal{E}_x^2 \int_{-\infty}^{\infty} F\{\beta\}\,\mathcal{K}x\,d\beta}{\mathcal{E}_y^2 \int_{-\infty}^{\infty} F\{\beta\}\,\mathcal{K}y\,d\beta}, \tag{5}$$

whereby variation of the tilt angle $\beta$ is manifested by a Gaussian distribution of the polymer about the mean tilt angle, $\mu$, with a standard deviation of $\sigma$, which reciprocally reflects the sample's order (7):

$$F\{\beta\} = \frac{1}{\sqrt{2\pi}\sigma}\, e^{-\frac{(\beta-\mu)^2}{2\sigma^2}}. \tag{6}$$

Thus lower values of $\sigma$ indicate a tighter distribution of the helix around the mean tilt angle. The explicit expression for the integrated absorption coefficients in the case of a Gaussian distribution are given in the Appendix. The standard deviation of the Gaussian function represents the disorder of the sample. The disorder is compound of several factors, e.g., imperfect Germanium (Ge) crystal, and imperfection of the lipid bilayer and incomplete reconstitution. As shall be shown later, one can estimate that disorder, using an x-ray rocking scan performed on the same sample.

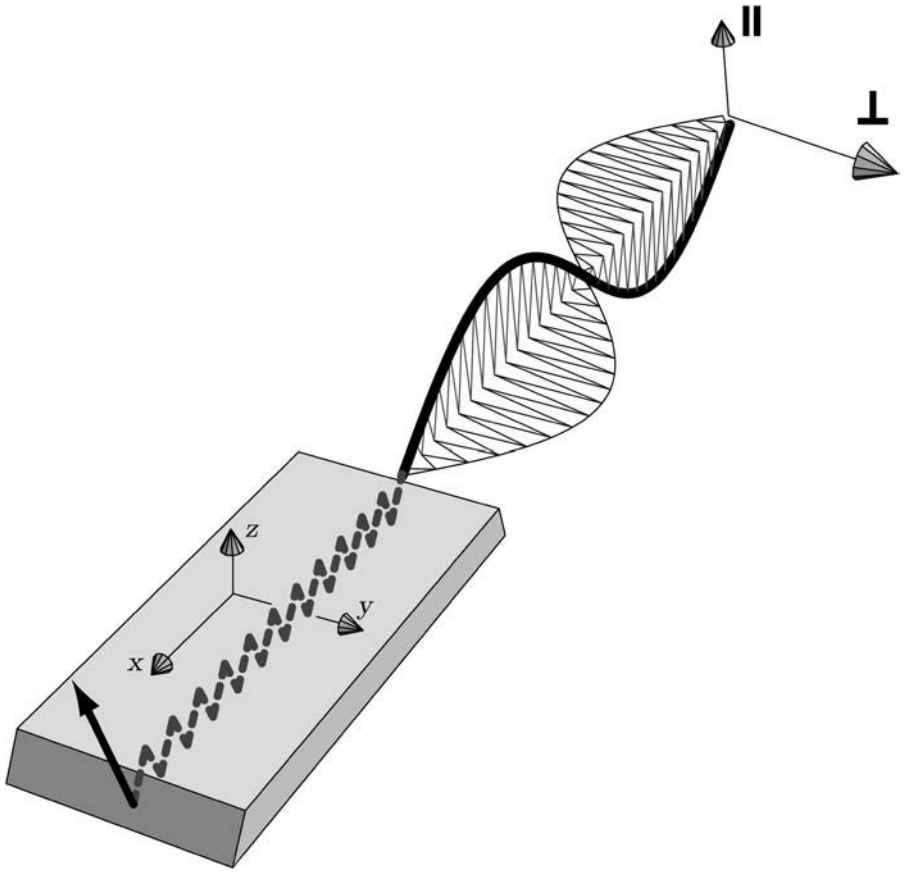


FIGURE 2 Geometrical configuration of ATR-FTIR according to Harrick (6). The two different polarizations are indicated as well as the sample axes.

## Angles extraction

Finding the three structural parameters describing a TDM's orientation, $\mu$, $\omega$, and $\sigma$, requires a set of three equations. Taking into account the measurements of $\mathcal{R}_{\text{polymer}}$ and $\mathcal{R}_{\text{site}}$, it is clear that an additional equation should be constructed. If the rotational difference between two site-specific labels is known ($\delta\Delta$), analyzing two polymers (each containing a single labeled site, and considering a constant $\mu$ for each site), these equations are obtained as

$$\mathcal{R}_{\text{helix}_\text{i}} = F\{\mu, \sigma_\text{i}\} \tag{7}$$

$$\mathcal{R}_{\text{site}_\text{i}} = F\{\mu, \sigma_\text{i}, \omega_\text{i}\} \tag{8}$$

$$\mathcal{R}_{\text{helix}_\text{j}} = F\{\mu, \sigma_\text{j}\} \tag{9}$$

$$\mathcal{R}_{\text{site}_\text{j}} = F\{\mu, \sigma_\text{j}, \omega_\text{i} + \delta\Delta\}, \tag{10}$$

whereby $\sigma_\text{i}$ and $\sigma_\text{j}$ reflect the fact that the disorder in both samples need not be equal.

Extracting $\mu$ from the measured polymer dichroism can also be done if the disorder is supplied. Thus, it is possible to calculate $\mu$, for each measured $\mathcal{R}_{\text{polymer}}$, as a function of a given disorder. Therefore, the effect of the disorder upon the outcome ($\mu$) can be tested, for specific values of $\mathcal{R}_{\text{polymer}}$. Similarly, it is possible to extract $\omega$ for a certain labeled position from the measured site dichroism given the polymer tilt, $\mu$, and the disorder. Thus, it is possible to calculate $\mu$ and $\omega$ in turn, for each measured $\mathcal{R}_{\text{polymer}}$, $\mathcal{R}_{\text{site}}$, and a given disorder.

## Transmembrane helices

The above theory is applicable to any rodlike-shaped polymer, and in particular to membranous proteins composed of $\alpha$-helices whereby the chromophore is the amide I vibration mode, mostly the peptidic C=O stretch (for review, see Ref. 8). The angle between the helix director and the transition dipole moment of the amide I mode, $\alpha$, is constant, and in the case of the amide I mode is equal to 39° (2). Furthermore, the rotational pitch angle, $\omega$, is defined as 0° when the helix's director, the membrane normal, and the transition dipole moment, all reside in the same plane. The rotational pitch angle, $\omega$, is specific for each of the amide I vibrations, and in a canonical helix the difference between $\omega_\text{i}$ and $\omega_{\text{i}+1}$ is 100°. When measuring the dichroism of the entire helix, and not a particular labeled site, $\omega$ is considered random, since its absorption arises from every amino acid along the helix backbone.

The site-specific label in an $\alpha$-helix normally consists of an 1-$^{13}$C=$^{18}$O that effectively resolves the amide I mode of the labeled site from the ''natural-abundance'' 1-$^{12}$C=$^{16}$O modes (9,10).

## MATERIALS AND METHODS

### Sample preparation

The peptide used in the experiments corresponded to residues $Met^{1}$–$Lys^{31}$ of HIV vpu (11,12): MQPIQIAIVALVVAIIIAIVVWSIVIIEYRK. Synthesis, purification, and reconstitution of the peptide in dimyristoylphosphatidylcholine (DMPC) lipid bilayers have been reported elsewhere in detail (13). Briefly, peptides were synthesized using standard F-moc chemistry. Purification was done by injecting the crude synthesis, dissolved in trifluoroacetic acid, into a Jupiter 5 C4-300 Å column (Phenomex, Cheshire, UK) equilibrated with 80% $H_2O$, 8% (w/v) acetonitrile and 12% (v/v) 2-propanol. Peptide elution was achieved with a linear gradient to a final solvent composition of 40% acetonitrile and 60% 2-propanol. All solvents contained 0.1% (v/v) trifluoroacetic acid. Finally the peptides were reconstituted into DMPC vesicles by co-solubilization in 1,1,1,3,3,3-hexafluoro-2-propanol (Merck, Whitehouse Station, NJ) followed by removal of the organic solvent and hydration.

### FTIR spectroscopy

FTIR spectra were recorded on a Nicolet Magna 560 spectrometer (Madison, WI). The spectrometer was equipped with a liquid nitrogen-cooled, high sensitivity MCT/A detector and was purged with $CO_2$ and water-depleted air. Attenuated total reflection (ATR) spectra were measured with a 25-reflection ATR accessory from Grasbey Specac (Kent, UK) and a wire grid polarizer (0.25 $\mu$M, Graseby Specac). Two-hundred microliters of sample (~2.5 mg/ml protein and 12.5 mg/ml lipid) were dried onto a Ge trapezoidal internal reflection element (50 × 2 × 10 mm). One-thousand interferograms were averaged for every sample and processed with 1.0 filling and Happ-Genzel apodization.

### X-ray scattering

For x-ray reflectivity measurements, the same sample used for the FTIR spectroscopy (peptide in DMPC deposited on a Ge surface), was used. The orientational distribution (mosaicity) of the oriented membrane stacks can be measured by a rocking scan or a $\chi$ scan. In a rocking scan, the sample is turned around an axis perpendicular to the plane of incidence. Thus, the angle of incidence $\alpha_i$ (measured between incoming beam and surface) and exit angle $\alpha_f$ is varied, while keeping the detector position fixed at $2\theta = \alpha_i + \alpha_f$, e.g., on the position of a Bragg peak $n2\pi/d = 4\pi/\lambda \sin\theta$. The intensity is peaked with a width corresponding to the tilt distribution (mosaicity) of lamellar domains. However, the maximum accessible tilt range limited by the absorbing substrate is only $2\theta$. Therefore, larger mosaicities are measured by $\chi$ scan where the sample is rocked around an axis in the plane of incidence, symmetrically around the specular position (see Fig. 4). Again the width of the peak (half-width at half-maximum) reflects the mosaicity, i.e., the distribution of local bilayer normal vectors.

Along with the rocking and $\chi$ scans, specular reflectivity scans ($\alpha_i = \alpha_f$) have been measured to assess the electron density profile of the bilayer. Reflectivity scans up to vertical momentum transfer $q_z = 4\pi/\lambda \sin\theta \simeq 1$ Å$^{-1}$ were taken at a sealed x-ray tube with Cu $K_\alpha$ radiation. The instrument was equipped with a curved *W/Si* multilayer optics for collimation obtained from Seifert Analytical X-Ray (Ahrensburg, Germany), a Huber diffractometer (Rimsting, Germany) and a fast scintillation counter (Cyberstar, Oxford Instruments, Witney, Oxfordshire, UK). The beam was parallel to $\sim\Delta\alpha_i \leq 0.01°$. From the reflectivity, the electron density profile was obtained by the Fourier synthesis method from the integrated peak intensities, using a Lorentz correction factor $1/q_z$, and phases (+, −, −, −, −). General aspects of reflectivity experiment and analysis are discussed in Salditt et al. (14).

## RESULTS

The results presented herein consist of an experimental system in which ATR-FTIR dichroism spectra were collected for the transmembrane domain of HIV vpu in lipid bilayers. Subsequently, the mosaicity of the sample was determined by an x-ray specular scan. In parallel, a computer-based simulation was constructed that calculates the affect of different mosaicities upon the calculated tilt and rotational pitch angle, given a measured dichroism.

### FTIR spectra

Typical ATR-FTIR spectra in both polarizations of the vpu transmembrane domain are shown in Fig. 3. The amide I vibrational mode is centered at 1655 cm$^{-1}$ with a peak-width at half-height of 23 cm$^{-1}$, both indicative of the high helical content of the protein (for review see Ref. 8). The dichroism of the helical amide I mode is 4.2, which indicates a high level of orientation relative to the bilayer plane (15).

### X-ray specular and $\chi$ scan

An x-ray specular scan of exactly the same sample used above in the FTIR analysis is depicted in Fig. 4. The unit spacing is of 55 Å, which corresponds to that expected of a DMPC bilayer in the gel phase (room level hydration) (16). An $\chi$ scan at the position of the first Bragg peak is depicted at the bottom of Fig. 4. The experimental data are readily fitted with a Gaussian curve, with a standard deviation of 2.1°.

### Simulations

To estimate the effects of sample disorder on the measured tilt and rotational pitch angles, a simulation was constructed.

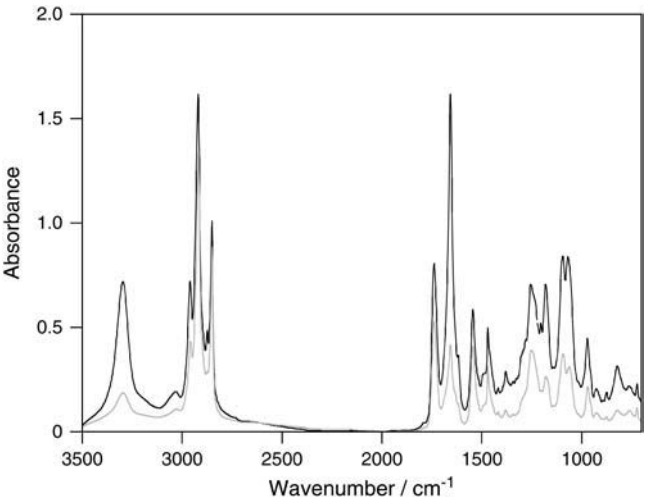


FIGURE 3 ATR-FTIR spectra of the vpu transmembrane domain reconstituted in DMPC vesicles. Spectra were obtained with parallel and polarized light depicted in solid and shaded lines, respectively. Careful examination of the results reveals that parallel and perpendicular peaks are centered at 1655 cm$^{-1}$, a characteristic peak of an $\alpha$-helix. This indicates a highly $\alpha$-helical structure of the peptide, as found previously in Kukol and Arkin (13).

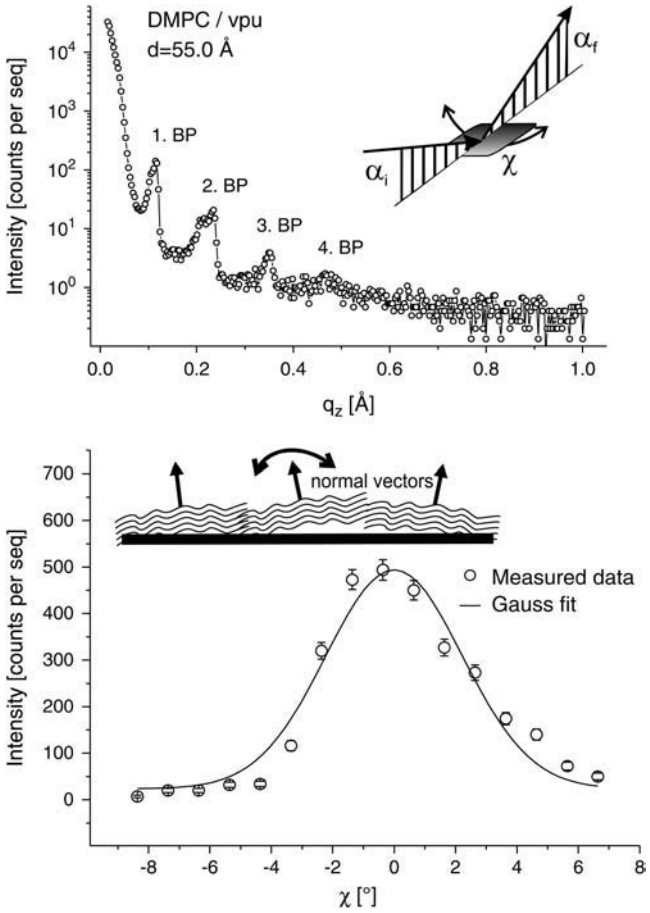


FIGURE 4 (*Top panel*) Specular scan of the multilamellar DMPC/vpu membranes in the gel phase at $T = 28$ C°, and $d = 55$ Å . The scattering geometry is shown in the inset. (*Bottom panel*) The $\chi$ scan on the first Bragg peak (i.e., at $\theta = 0.35°$). The scan measured at this peak is fitted to a Gaussian mosaicity function with $\sigma = 2.1°$, and is a measure for the probability distribution of local membrane normal vectors (see *sketch* in *inset*).

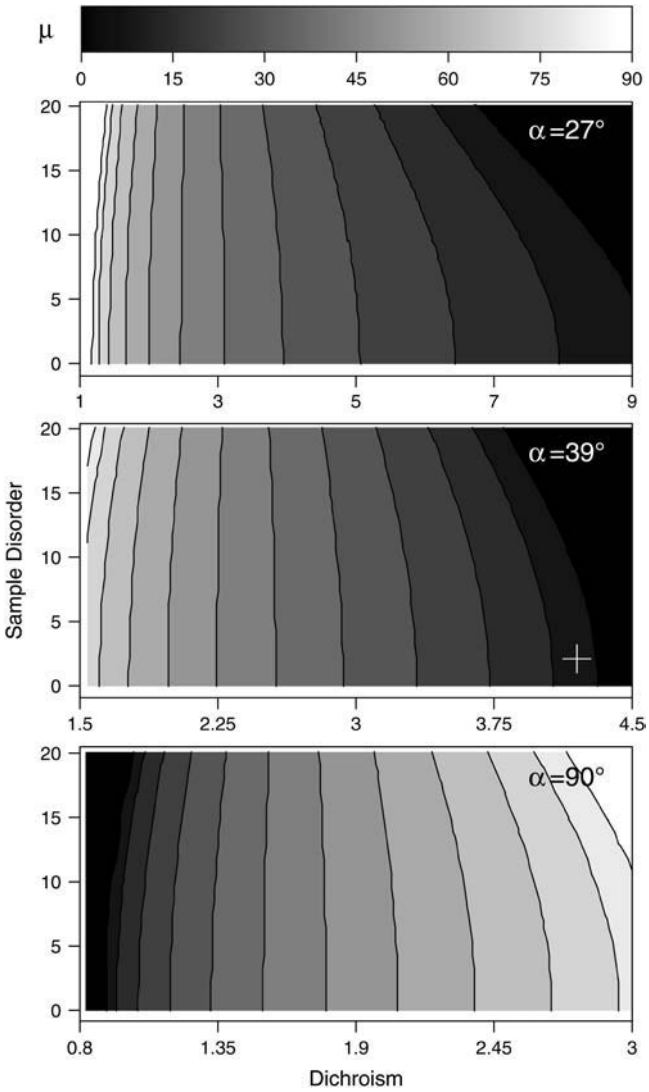


FIGURE 5 The calculated mean tilt angle $\mu$, as a function of the measured dichroism and sample disorder. The uppermost panel (the *grayscale bar*) represents the value of $\mu$ used in the lower panels. On the continuous scale, black indicates 0° whereas white indicates 90°. (*Top panel*) Data for the amide A vibrational mode in which $\alpha = 27°$. (*Middle panel*) Data for the amide I vibrational mode in which $\alpha = 39°$. (*Bottom panel*) Data for the lipid $CH_2$ stretching vibrational mode in which $\alpha = 90°$. Each panel is divided into 12 equally spaced contours. The experimental measurement of the transmembrane domain of HIV vpu is indicated by a cross in the middle panel (the amide I vibrational mode).

The simulations correspond to that obtained in ATR-FTIR, employing the thick film approximation and an internal reflection element made out of Ge (17). The refractive index of the lipid bilayer and Ge were taken as 1.43 and 4.0, respectively (18,19,20,21).

### *Tilt angles*

Fig. 5 depicts the derived tilt angle as a function of the dichroism and different sample disorders. The results are shown for three different vibrational modes: 1), the amide A mode (the peptidic N-H stretch) with an $\alpha = 27°$; 2) the amide I mode (mostly the peptidic C=O stretch) with an $\alpha = 39°$; and 3), the lipid methylene stretching mode with an $\alpha = 90°$ (8).

The data in Fig. 5 indicate that relatively small values of disorder have little effect on the calculated tilt angle:

1. Differences between disorders of $\sigma = 5°$ and $\sigma = 0°$ resulted in a tilt ambiguity smaller than 1.5° for all values of $\mathcal{R}_{\text{polymer}}$. If one excludes extreme amide A dichroisms ($\mathcal{R}_{\text{polymer}} \geq 8.3$), the derived differences in the calculated tilt angle are even smaller than 1°.
2. Differences between disorders of $\sigma = 10°$ and $\sigma = 0°$ resulted in a tilt ambiguity smaller than 4° for most values of $\mathcal{R}_{\text{polymer}}$. This excludes $\mathcal{R}_{\text{polymer}} \geq 8$ for amide A (5.2° to 8.7°), and $\mathcal{R}_{\text{polymer}} \cong 4.1$ for amide I (up to 5°).
3. Differences between disorders of $\sigma = 20°$ and $\sigma = 10°$ resulted in a significant changes in the calculated tilt values – up to 16° (10° for lipids).

Fig. 5 enables us to directly calculate the tilt angle for a given dichroism and disorder. Specifically it is possible to interpret the experimental data in which the measured dichroism of the helix was 4.2 and the disorder measured by the x-ray specular rocking scan was $\sigma = 2.1°$. Taken together the derived tilt angle is $\beta = 9°$, a value similar to that obtained using multiple site-specific labels of $\beta = (6.5 \pm 1.7)°$ (13). However, in contrast to the previous study, in the current measurement there was no need to measure peptides that are isotopically labeled to derive the same tilt. Moreover the previous derivation using site-specific labels (13) included an assumption that the rotational pitch angle difference between the two labeled sites was $\Delta\omega = 100°$. In the current measurement no such assumption is needed.

### *Rotational pitch angles*

Fig. 6 depicts the influence of the disorder on the derived rotational pitch angles for several different helical tilts. Here only the amide I vibrational mode is used since it is the most common site-specific isotope label used in FTIR spectroscopy (10).

The data indicate, as in the case of helical tilt $\beta$, that relatively small values of disorder have little effect on the calculated rotational pitch angle $\omega$:

1. Differences between disorders of $\sigma = 5°$ and $\sigma = 0°$ resulted in a change smaller than 3° for all values of $\mathcal{R}_{site}$, excluding extreme dichroism values ($\mathcal{R}_{site} = 10.4$ assuming a tilt angle of $\beta = 10°$). For larger tilt angles the effect of the disorder is even smaller: only up to 2° and 1° for $\beta = 10°$ and 20°, respectively.
2. Differences between disorders of $\sigma = 10°$ and $\sigma = 0°$ resulted in a change smaller than 10°, 5°, and 3.4° for $\beta = 10°$, 15°, and 20°, respectively. This excludes extreme dichroism values such as $\mathcal{R}_{site} = 10.1$ for $\beta = 10°$ (19°) and $\mathcal{R}_{site} = 10.7$ for $\beta = 15°$ (5.7°).
3. Differences between disorders of $\sigma = 20°$ and $\sigma = 0°$ resulted in a significant change in $\omega$ for $\beta = 5°$ and 10° – up to 52° and 24°, respectively. However, for $\beta = 15°$ and 20°, the maximal change is bounded by 15° and 10°, respectively.

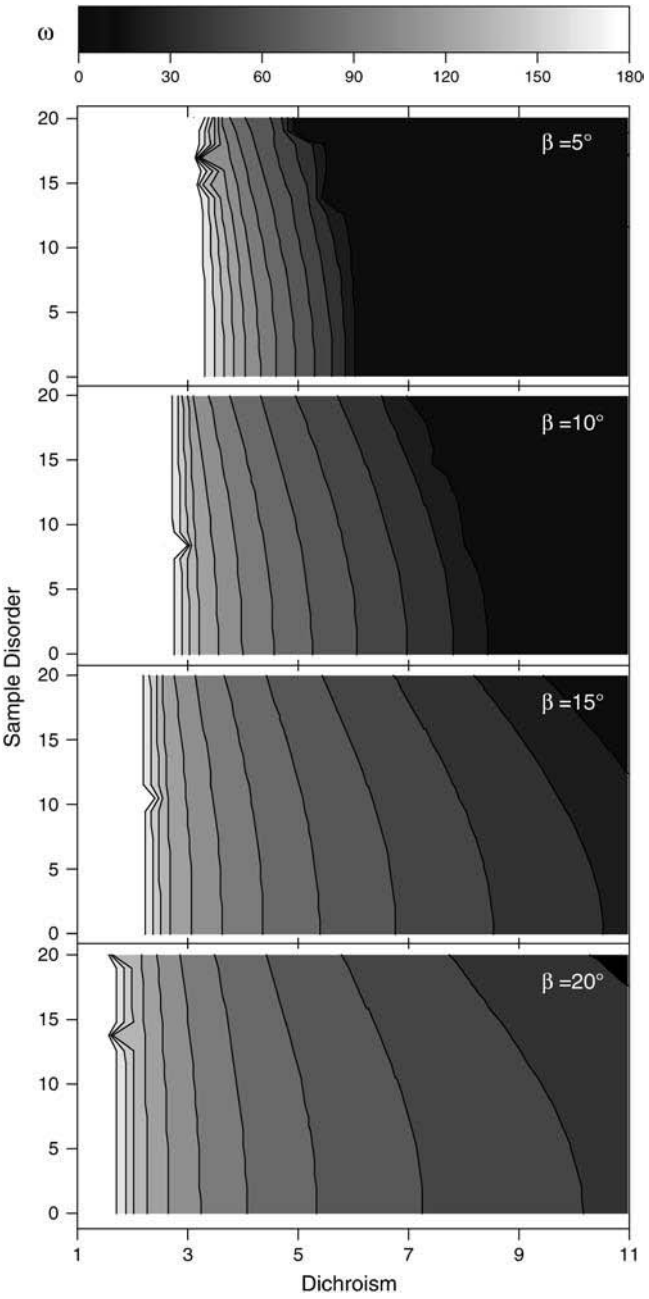


FIGURE 6 The calculated rotational pitch angle, $\omega$, as a function of the measured dichroism for different sample disorders, $\sigma$, as indicated. The amide I vibrational mode ($\alpha = 39°$) is used in all of the calculations. The uppermost panel (the *black-to-white bar*) represents the value of $\omega$ used in the lower panels. On the continuous scale, black indicates 0° whereas white indicates 90°. The different panels are calculated for different tilt angles, as indicated. Each panel is divided into 12 equally spaced contours.

## DISCUSSION

The current study aims to determine the information content in linear dichroism studies. Specifically, how does sample inhomogeneity reduce the accuracy of the derived tilt angle, and moreover, how does the magnitude of the inaccuracy depend on the polymer tilt? The same questions pertain to the second aspect of the work, addressing not the polymer tilt, but rather its rotational pitch angle determined by site-directed dichroism, given a polymer tilt.

Close inspection of the results of Fig. 5 enables us to answer the first set of questions. In Fig. 7 we can see that neglecting disorders $\leq 5°$ would only the affect the calculated tilt angle by 1° at most. Furthermore, neglecting disorders $\leq 10°$ would change $\beta$ by 4° at most. These values are well within experimental errors using IR spectroscopy (as reported in 9,13,22–28). Therefore, neglecting disorders $\sigma \leq 10°$ and especially $\sigma \leq 5°$ would have little effect on the measurement accuracy of the polymer orientation.

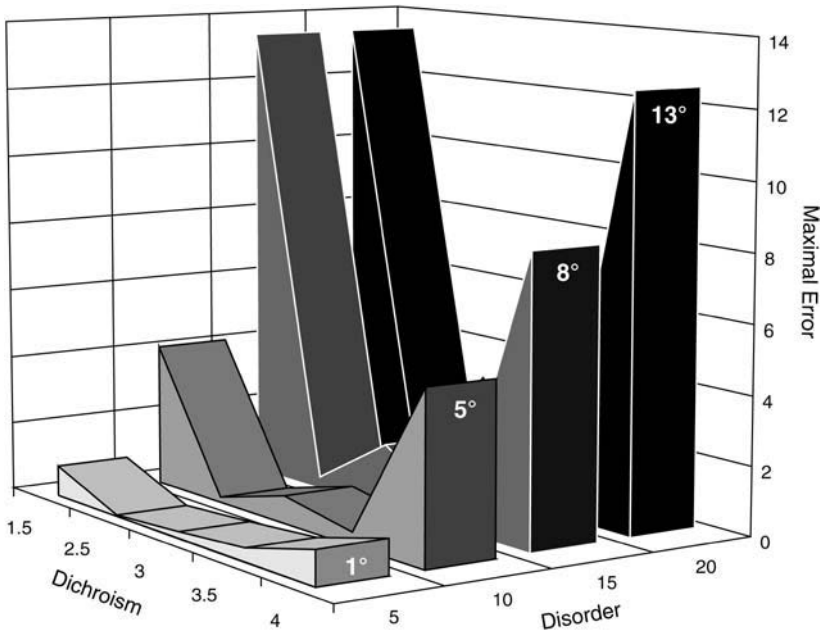


FIGURE 7 The maximal errors in the calculated tilt angle as a function of disorder negligence for the amide I vibrational mode.

Figs. 6 and 8 enable us to answer the second set of questions. In Fig. 8 we can see that neglecting disorders $\sigma \leq 5°$ would change the calculated rotational pitch angle by only $\leq 3.4°$ (in the case of $\beta = 15°$). These values are well within the experimental error range. In instances of higher tilts, neglecting the disorder would change $\omega$ even by less.

In the case of a lower tilt ($\beta = 10°$), the maximal error would be 4.6°, a value still well within the experimental error range. However, for the extreme $\mathcal{R}_{site} \geq 10$ (values that are experimentally rare), the respective change is 10.8°. To conclude, excluding few cases, disorders $\leq 10°$ are ''acceptable'', and negligible for disorders $\leq 5°$, considering standard experimental errors.

Taken together it is possible to reach the following conclusions:

1. When the sample is ''reasonably'' deposited, i.e., its disorder is $<10°$, the effect of the disorder on both the calculated tilt and rotational angles is relatively insignificant.
2. When disorders are $\leq 5°$, the effect of the disorder is negligible.
3. It is far more important to measure the dichroism accurately than it is to estimate the disorder – changes in the calculated dichroism has significantly bigger effect than the disorder.

The computer-based simulations that are used here are derived from the same calculations used in previous results (7). Here, we used these calculations to extract the disorder or dichroic ratio from a given tilt angle, and not vice versa; however, it is mathematically equivalent. The computational approach presented here has therefore been compared with independent data for several results.

We examined possible generalizations for the disorder effect, none of which yielded an acceptable match. However, when approximating the effect of the disorder for a specific dichroic value, a linear correlation was found between $\cos^2(\sigma)$ and the gradient effect of the disorder on the value of the tilt angle, $\beta$. This result is not definite, and the match found is valid for only a narrow range of dichroic values. Moreover, the experimental $\mathcal{R}_{helix}$ and $\mathcal{R}_{site}$ values are usually not within that range, and therefore the approximation is not readily applicable. In contrast, the computational approach presented here is unambiguous and considers the entire range of possible $\mathcal{R}_{helix}$ and $\mathcal{R}_{site}$ values.

The theory presented here is derived mathematically from well-known physical principles. When applying it to experimental results, several factors might affect the accuracy of the measurement: Noise in the absorption level; nonperfect polarization state; reactions between the internal reflection element and the substrate; nonperfectly isotopic sample; and inaccuracies in the angle of incidence (assumed here 45°). However, according to Axelsen et al. (29), the effects of these factors contribute a relatively small amount of error to experimental measurements. An additional factor that might cause such inaccuracies is $n_2$, here chosen to be 1.43. We examined the effect of deviations from this value on the dichroic ratio, and found that deviations within the range of 0.03 from 1.43 have very little effect on $\mathcal{R}$, and therefore on $\beta$ and $\sigma$ (data not shown). Values of 1.4–1.46 for $n_2$ are widely acceptable (1,18,19,21).

Finally we present a simple approach to measure the polymer (e.g., helix) tilt using a combination of FTIR dichroism and x-ray specular rocking scans. Using the dichroism derived from the FTIR spectra combined with the

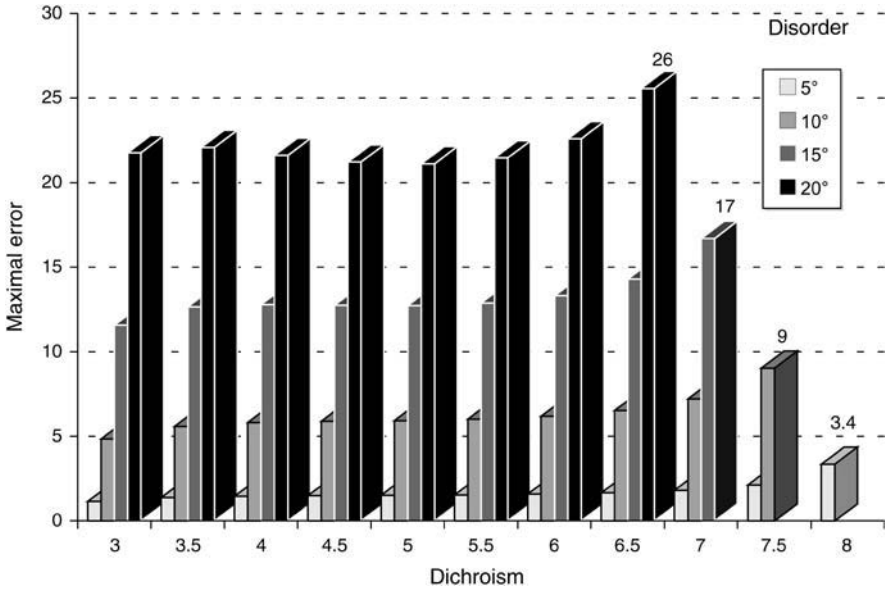


FIGURE 8 The changes in the calculated rotational pitch angle, $\omega$ as a function of disorder negligence assuming a tilt angle of $\beta = 15°$.

sample mosaicity measured from the x-ray scans it is possible to directly derive the polymer tilt. Moreover, to our knowledge this represents the first instance in which a precise measurement (as opposed to an order parameter) of a transmembrane helix tilt was obtained from infrared spectroscopy without the need for isotopic labeling.

## APPENDIX

The values of the axial electric field components in the case of the thick film approximation are, according to Harrick (6),

$$\mathcal{E}_x = \frac{2\cos(\varphi)(\sin(\varphi)^2 - n_{21}^2)^{1/2}}{(1-n_{21}^2)^{1/2}[(1+n_{21}^2)\sin(\varphi)^2 - n_{21}^2]^{1/2}}, \tag{A1}$$

$$\mathcal{E}_y = \frac{2\cos(\varphi)}{(1-n_{21}^2)^{1/2}}, \tag{A2}$$

$$\mathcal{E}_z = \frac{2\cos(\varphi)\sin(\varphi)}{(1-n_{21}^2)^{1/2}[(1+n_{21}^2)\sin(\varphi)^2 - n_{21}^2]^{1/2}}, \tag{A3}$$

where $\phi$ is the angle of incidence between the infrared beam and the internal reflection element (45°), and $n_{21}$ is the ratio between the refractive indices of the sample ($n_2 = 1.43$) and the internal reflection element ($n_1 = 4.0$).

In the case of Ge internal reflection element, the values are $\mathcal{E}_x = 1.398$, $\mathcal{E}_y = 1.516$, and $\mathcal{E}_z = 1.625$. The integrated absorption coefficients in case of a Gaussian distribution were derived in Kass et al. (7). In the case of a unique site (i.e., dependence on the rotational pitch angle, $\omega$):

$$\mathcal{K}x\{\omega\} = \frac{\cos(\alpha)^2\left(\frac{1}{2} - \frac{\cos(2\mu)}{2e^{2\sigma^2}}\right)}{2} + \frac{\left(\frac{1}{2} + \frac{\cos(2\mu)}{2e^{2\sigma^2}}\right)\cos(\omega)^2\sin(\alpha)^2}{2} + \frac{\cos(\alpha)\cos(\mu)\cos(\omega)\sin(\alpha)\sin(\mu)}{e^{\sigma^2}} + \frac{\sin(\alpha)^2\sin(\omega)^2}{2}, \tag{A4}$$

$$\mathcal{K}y\{\omega\} = \mathcal{K}x(\omega), \tag{A5}$$

$$\mathcal{K}z\{\omega\} = \cos(\alpha)^2\left(\frac{1}{2} + \frac{\cos(2\mu)}{2e^{2\sigma^2}}\right) + \left(\frac{1}{2} - \frac{\cos(2\mu)}{2e^{2\sigma^2}}\right)\cos(\omega)^2\sin(\alpha)^2 - \frac{2\cos(\alpha)\cos(\mu)\cos(\omega)\sin(\alpha)\sin(\mu)}{e^{\sigma^2}}. \tag{A6}$$

By integrating the results of Eqs. 14–16 throughout all possible rotational pitch angles $\omega$, we obtain the equations for the integrated absorption coefficients for a helix, modeling the sample disorder as a Gaussian distribution:

$$\mathcal{K}x\{\langle\omega\rangle\} = \frac{\cos(\alpha)^2\left(\frac{1}{2} - \frac{\cos(2\mu)}{2e^{2\sigma^2}}\right)}{2} + \frac{\sin(\alpha)^2}{4} + \frac{\left(\frac{1}{2} + \frac{\cos(2\mu)}{2e^{2\sigma^2}}\right)\sin(\alpha)^2}{4}, \tag{A7}$$

$$\mathcal{K}y\{\langle\omega\rangle\} = \mathcal{K}x\{\langle\omega\rangle\}, \tag{A8}$$

$$\mathcal{K}z\{\langle\omega\rangle\} = \cos(\alpha)^2\left(\frac{1}{2} + \frac{\cos(2\mu)}{2e^{2\sigma^2}}\right) + \frac{\left(\frac{1}{2} - \frac{\cos(2\mu)}{2e^{2\sigma^2}}\right)\sin(\alpha)^2}{2}. \tag{A9}$$

This research was supported in part by a grant from the Israel Science Foundation (No. 784/01) to I.T.A., and grants from the Deutsche Forschungsgemeinschaft and from Niedersachsen to I.T.A. and T.S.

## REFERENCES


1. Axelsen, P. H., and M. J. Citra. 1996. Orientational order determination by internal reflection infrared spectroscopy. *Prog. Biophys. Mol. Biol.* 66:227–253.
2. Tsuboi, M. 1962. Infrared dichroism and molecular conformation of A-form poly-g-benzyl-L-glutamate. *J. Polym. Sci. B.* 59:139–153.
3. Marsh, D., M. Muller, and F. J. Schmitt. 2000. Orientation of the infrared transition moments for an $\alpha$-helix. *Biophys. J.* 78:2499–2510.
4. Fraser, R. D. B. 1953. The interpretation of infrared dichroism in fibrous protein structures. *J. Chem. Phys.* 70:1511–1515.
5. Fraser, R. D. B. 1958. Interpretation of infrared dichroism in axially oriented polymers. *J. Chem. Phys.* 28:1113–1115.
6. Harrick, N. 1967. Internal Reflection Spectroscopy, 1st Ed. Interscience Publishers, New York.
7. Kass, I., E. Arbely, and I. T. Arkin. 2004. Modeling sample disorder in site-specific dichroism studies of uniaxial systems. *Biophys. J.* 86: 2502–2507.
8. Braiman, M. S., and K. J. Rothschild. 1988. Fourier transform infrared techniques for probing membrane protein structure. *Annu. Rev. Biophys. Biophys. Chem.* 17:541–570.
9. Torres, J., P. D. Adams, and I. T. Arkin. 2000. Use of a new label, $^{13}C{=}^{18}O$, in the determination of a structural model of phospholamban in a lipid bilayer. Spatial restraints resolve the ambiguity arising from interpretations of mutagenesis data. *J. Mol. Biol.* 300:677–685.
10. Torres, J., A. Kukol, J. M. Goodman, and I. T. Arkin. 2001. Site-specific examination of secondary structure and orientation determination in membrane proteins: the peptidic $^{13}C{=}^{18}O$ group as a novel infrared probe. *Biopolymers.* 59:396–401.
11. Strebel, K., T. Klimkait, and M. A. Martin. 1988. A novel gene of HIV-1, vpu, and its 16-kiloDalton product. *Science.* 241:1221–1223.
12. Cohen, E. A., E. F. Terwilliger, J. G. Sodroski, and W. A. Haseltine. 1988. Identification of a protein encoded by the vpu gene of HIV-1. *Nature.* 334:532–534.
13. Kukol, A., and I. T. Arkin. 1999. Vpu transmembrane peptide structure obtained by site-specific Fourier transform infrared dichroism and global molecular dynamics searching. *Biophys. J.* 77:1594–1601.
14. Salditt, T., C. Li, A. Spaar, and U. Mennicke. 2002. X-ray reflectivity of solid-supported, multilamellar membranes. *Eur. Phys. J.* E7:105–116.
15. Vigano, C., L. Manciu, F. Buyse, E. Goormaghtigh, and J. M. Ruysschaert. 2000. Attenuated total reflection IR spectroscopy as a tool to investigate the structure, orientation and tertiary structure changes in peptides and membrane proteins. *Biopolymers.* 55:373–380.
16. Salditt, T. 2003. Lipid-peptide interaction in oriented bilayers probed by interface-sensitive scattering methods. *Curr. Opin. Struct. Biol.* 13:467–478.
17. Silvestro, L., and P. H. Axelsen. 1998. Infrared spectroscopy of supported lipid monolayer, bilayer, and multibilayer membranes. *Chem. Phys. Lipids.* 96:69–80.
18. Frey, S., and L. K. Tamm. 1991. Orientation of melittin in phospholipid bilayers. A polarized attenuated total reflection infrared study. *Biophys. J.* 60:922–930.
19. Picard, F., T. Buffeteau, B. Desbat, M. Auger, and M. Pezolet. 1999. Quantitative orientation measurements in thin lipid films by attenuated total reflection infrared spectroscopy. *Biophys. J.* 76:539–551.
20. Citra, M. J., and P. H. Axelsen. 1996. Determination of molecular order in supported lipid membranes by internal reflection Fourier transform infrared spectroscopy. *Biophys. J.* 71:1796–1805.
21. Brauner, J. W., R. Mendelsohn, and F. G. Prendergast. 1987. Attenuated total reflectance Fourier transform infrared studies of the interaction of melittin, two fragments of melittin, and $\delta$-hemolysin with phosphatidylcholines. *Biochemistry.* 26:8151–8158.
22. Arkin, I. T., K. R. MacKenzie, and A. T. Brunger. 1997. Site-directed dichroism as a method for obtaining rotational and orientational constraints for oriented polymers. *J. Am. Chem. Soc.* 119:8973–8980.
23. Kukol, A., P. D. Adams, L. M. Rice, A. T. Brunger, and T. I. Arkin. 1999. Experimentally based orientational refinement of membrane protein models: a structure for the Influenza A M2 $H^+$ channel. *J. Mol. Biol.* 286:951–962.
24. Torres, J., A. Kukol, and I. T. Arkin. 2000. Use of a single glycine residue to determine the tilt and orientation of a transmembrane helix. A new structural label for infrared spectroscopy. *Biophys. J.* 79:3139–3143.
25. Torres, J., and I. T. Arkin. 2002. C-deuterated alanine: a new label to study membrane protein structure using site-specific infrared dichroism. *Biophys. J.* 82:1068–1075.
26. Kukol, A., and I. T. Arkin. 2000. Structure of the Influenza C virus CM2 protein transmembrane domain obtained by site-specific infrared dichroism and global molecular dynamics searching. *J. Biol. Chem.* 275:4225–4229.
27. Torres, J., J. A. Briggs, and I. T. Arkin. 2002. Multiple site-specific infrared dichroism of CD3-$\zeta$, a transmembrane helix bundle. *J. Mol. Biol.* 316:365–374.
28. Kukol, A., J. Torres, and I. T. Arkin. 2002. A structure for the trimeric MHC class II-associated invariant chain transmembrane domain. *J. Mol. Biol.* 320:1109–1117.
29. Axelsen, P. H., B. K. Kaufman, R. N. McElhaney, and R. N. Lewis. 1995. The infrared dichroism of transmembrane helical polypeptides. *Biophys. J.* 69:2770–2781.